# Calix[4]crowns with perfluoroalkylsulfonylcarboxamide functions: a complexation approach for heavy group 2 metal ions

Reissig, F.; Bauer, D.; Al-Ameed, K.; Luber, S.; Köckerling, M.; Steinbach, J.; Pietzsch, H.-J.; Mamat, C.;

Originally published:

January 2023

**Inorganic Chemistry Frontiers 10(2023), 370-382**

DOI: https://doi.org/10.1039/d2qi01637k

ARTICLE

# Calix[4]crowns with perfluoroalkylsulfonylcarboxamide functions: a complexation approach for heavy group 2 metal ions

Received 00th January 20xx,
Accepted 00th January 20xx

DOI: 10.1039/x0xx00000x

Falco Reissig,[a,b] David Bauer,[a,b,†] Karrar Al-Ameed,[c,#] Sandra Luber,[c] Martin Köckerling,[d,e] Jörg Steinbach,[a,b] Hans-Jürgen Pietzsch [a,b] and Constantin Mamat [*a,b]

Heavy alkaline earth metals offer radionuclides which are promising candidates for radiopharmaceutical applications like the γ-emitter barium-131 for diagnosis or the alpha-emitters radium-223/-224 – with similar chemical properties to barium – for targeted alpha-particle therapy. However, there is a lack of suitable chelation agents, especially for these metal ions. A series of calix[4]crown-6 derivatives with perfluoroalkylsulfonylcarboxamide functions ($R_F$ = $CF_3$, $C_2F_5$, *i*-$C_3F_7$, *n*-$C_4F_9$) was synthesized to serve as cage-like chelators for $Ba^{2+}$ and $Ra^{2+}$ to determine the complexation behaviour. These functional ligands are deprotonated even at slightly acidic pH due to the intense electron withdrawing effect of the sulfonamide groups. The obtained ligands were easily converted to the desired barium complexes as well as into calix-crown compounds containing two sodium ions. DFT calculation methods were used to discover either the binding behavior of the metal ions with the desired ligands as well as the influence of the different donor groups from the chelating moiety of the calixarenes with respect to different pH. Radiolabeling procedures with the radionuclides barium-133 and radium-224 as [$^{133}$Ba]$BaCl_2$ and [$^{224}$Ra]$Ra(NO_3)_2$ were performed to determine association constant values between 4.1 and 8.2 for the appropriate $M^{2+}$ complexes using a two-phase extraction procedure. A stability test using physiological $Ca^{2+}$ solution showed a minor release of approx. 1–7% of the central ions ($Ba^{2+}$ respectively $Ra^{2+}$) from the complexes.

## Introduction

Calixarenes[1,2] are known to be suitable chelating agents not only for main group metal ions,[3] but also for transition metal ions, anions and uncharged (small) molecules such as pharmaceuticals and natural compounds.[4,5] Other applications involve the functionalization of nanoparticles, the mediation as catalyst[6-8] or the determination of cations[9] or anions[10] as chemical sensors for quantifications.[11,12] Thus, a large variety of special functionalized calixarenes was prepared to serve as molecular containers for organic and inorganic ions. Especially, the combination of crown ethers and calixarenes is beneficial for this purpose.[13-15] The so called calixcrowns, in contrast to unmodified or open-chained calixarenes, lead to increased complex stabilities resulting in higher stability constants and higher selectivity for certain metal cations.[16]

Generally, a radiometal-based radiotracer consists of a chelating system to strongly cage the radiometal and a connected targeting moiety of high affinity and selectivity to safely transfer the radiotracer to the organ or tissue of choice.[17] Importantly, high complex stabilities are required to avoid the release of the radiometal from the resulting complex *in vivo* and thus an uncontrolled distribution and accumulation in the body which can lead to inadequate images or treat the healthy tissue.[18] Ligands for a sufficient binding of group 2 (radio)metal ions like $Sr^{2+}$, $Ba^{2+}$ [19] or $Ra^{2+}$ [20-22] for the use in radiopharmaceutical applications are known, but did not lead to any successful outcome so far.[23,24]

Several radioisotopes of radiopharmaceutical interest are known from barium.[25,26] Due to the suitable half-life of 11.5 days and a gamma emission of 124 keV (30%), barium-131 is found to be a good candidate for diagnostic purposes.[27] Additionally, the nonradioactive isotopes of barium serve as a surrogate for basic investigations by NMR or UV-Vis in the development of radium-223/-224-based radiopharmaceuticals.[28-31] The appropriate half-lives ($^{223}$Ra: 11.4 d; $^{224}$Ra: 3.6 d)[32,33] and nuclear decay properties make these two radionuclides useful tools in targeted radionuclide therapy with α-particles.[34] Until now, [$^{223}$Ra]$RaCl_2$ (Xofigo®) is the only EMA and FDA approved radiopharmaceutical for α-therapeutic applications in the clinic.[35] However, radium solely administered in its ionic form preferentially addresses the bone tissue. The same behavior is anticipated for [$^{131}$Ba]$Ba^{2+}$ due to its comparable calcimimetic behavior.[25,26] In addition, the combination of the gamma emitter $^{131}$Ba for diagnosis and the both alpha emitters

[a] *Helmholtz-Zentrum Dresden-Rossendorf, Institut für Radiopharmazeutische Krebsforschung, Bautzner Landstraße 400, D-013228 Dresden, Germany.*
[b] *TU Dresden, Fakultät Chemie und Lebensmittelchemie, D-01062 Dresden, Germany.*
[c] *University of Zurich, Department of Chemistry, Winterthurerstrasse 190, CH-8057 Zurich, Switzerland.*
[d] *Universität Rostock, Institut für Chemie – Anorganische Festkörperchemie, Albert-Einstein-Straße 3a, D-18059 Rostock, Germany.*
[e] *Universität Rostock, Department Life, Light and Matter, D-18051 Rostock, Germany.*
† Current address: Memorial Sloan Kettering Cancer Center, Molecular Pharmacology Program, 1275 York Avenue, New York, NY 10065, USA.
# Current address: University of Kufa, Department of Chemistry, Najaf 54001, Iraq.
Electronic Supplementary Information (ESI) available: NMR spectra of compounds, details of the DFT calculations. See DOI: 10.1039/x0xx00000x

$^{223/224}$Ra for therapy is beneficial and leads to a matched nuclide pair[36] for a theranostic approach.[37,38]

Functionalized calix[4]crown ethers and their complexes with $Ba^{2+}$ and $Ra^{2+}$ are known from the literature,[24,28-30,39,40] e.g., in environmental chemistry, but little is known about the complexation behavior, the respective complex stability constants, and the *in vivo* behavior of such complexes. In the past, the cavity size of calix[4]crown-6 was tested to fit best for heavier group 2 metals.[41-44] Extraction studies with these calix compounds and the desired (radio)metal ions are a convenient way allowing the determination of the respective stability complex constants.

The big challenge is to use both divalent ions to address other oncological targets than the bones. Therefore, the design of highly stable chelate complexes is essential. The aim of this investigation comprises the synthesis of calix[4]crown-6 ethers containing easy deprotonable groups at physiological pH for the strong and selective complexation especially of $Ba^{2+}$ and $Ra^{2+}$. Recently, we found the highest complexation constants for functionalized calix[4]crown-6-complexes containing a *N*-(trifluoromethyl)sulfonylcarboxamide unit.[28] Therefore, the two remaining OH groups of the calix[4]crown-6-scaffold were functionalized with different perfluoroalkylsulfonylcarboxamide moieties.[31] These groups are necessary to stably bind $Ba^{2+}$ and $Ra^{2+}$ with good selectivity over the lighter group 2 metal ions $Mg^{2+}$ and $Ca^{2+}$. The binding behavior of the considered ions to the crown ether cage and the sulfonamide side chains of the calix[4] ligands was determined by in silico methods based on DFT calculations. Thereby, the influence of the chain length and thus the impact of the electron withdrawing character combined with the different steric demand of these perfluoroalkyl residues ($CF_3$, $C_2F_5$, *i*-$C_3F_7$ and $C_4F_9$) in dependence on the association constants was explored in combination with the influence of the groups (H vs. $^t$Bu) at the upper rim of the calix skeleton. Due to the higher electron withdrawal and a higher steric demand of the perfluorinated groups, it is more convenient to create a negative charge by deprotonation and thus a hard basic center even at the physiological pH value. Moreover, the ligand-ion-interaction was examined by performing extraction studies with a two-phase chloroform-water system and the radionuclides [$^{133}$Ba]$Ba^{2+}$ and [$^{224}$Ra]$Ra^{2+}$. Results of the barium investigations with the nonradioactive isotopes will give the basis for the formation behavior of the respective radium complexes.

## Results and discussion

### Syntheses of functionalized calix[4]arenes

Two sets of calixarenes with and without *tert*-butyl groups on the upper rim (to provide more flexibility on the calix skeleton) were prepared containing aliphatic sulfonylcarboxamides in the side chain. For this purpose, the starting materials H-calix[4]crown-6 (**1**) as well as *tert*-butyl-calix[4]crown-6 (**2**) were reacted with ethyl bromoacetate to introduce the side chains. Both resulting di-esters **3** and **4** were hydrolyzed to give the free

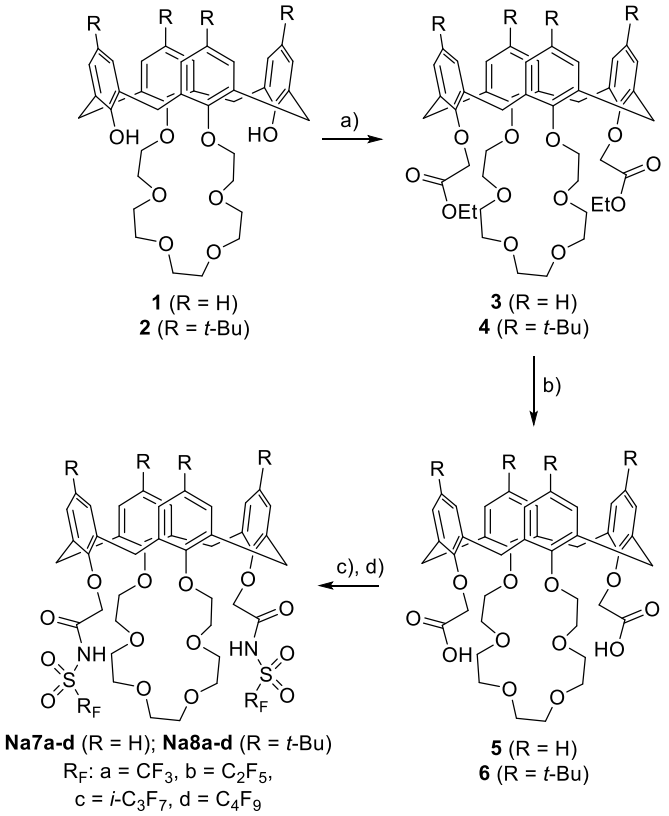


**Scheme 1.** Preparation of the calix[4]arenes **Na7a-d** and **Na8a-d** containing the aliphatic perfluorosulfonylcarboxamide groups. *Reagents and conditions:* a) $BrCH_2COOEt$, NaI, 50°C, overnight; b) $Me_4NOH$, THF-$H_20$, 7-16 h; c) oxalyl chloride, $CCl_4$, 65°C, 5 h; d) sulfonamide, NaH, dichloromethane, rt, overnight.

di-acids **5** and **6**, respectively. Afterwards, both di-acids **5** and **6** were converted into the di-acid chlorides with oxalyl chloride and were further reacted with the respective perfluoroalkylsulfonamides ($R_F$ = $CF_3$, $C_2F_5$, i-$C_3F_7$, $C_4F_9$ after subsequent deprotonation with NaH in dichloromethane at ambient temperature. After conventional aqueous workup and purification, the desired calixarenes were obtained as uncharged disodium complexes **Na7a-d** and **Na8a-d** were obtained in 26-77% yield (Scheme 1).

The existence of the disodium-complexes was evidenced by the results of two X-ray single crystal structure analyses of compounds **Na8b** and **Na8d**. Both molecular structures are presented in Figure 1. It was found, that both amide functions are subjected to amide-iminol-tautomerism (discussed in detail later) as shown in Scheme 2, are afterwards deprotonated at the OH group (iminol form) under aqueous conditions at pysiological pH, and are thus able to form the respective neutral complexes **Na8b** and **Na8d** with two $Na^+$ ions.

In both complexes, the $Na^+$ ions are located inside the cavity and are coordinated by the oxygen atoms of the crown ether moiety and the oxygen atoms of the tautomeric carboxamide functions. The diameters of both crown ether rings in **8b** and **8d** are expanded at the sites where they are attached to the tetraphenyl cages. The O···O distances are much longer than the usual O···O distances, found in 18-crown-6 molecules. They are found in the range of 2.6–2.8 Å, whereas, e.g. the O1···O6

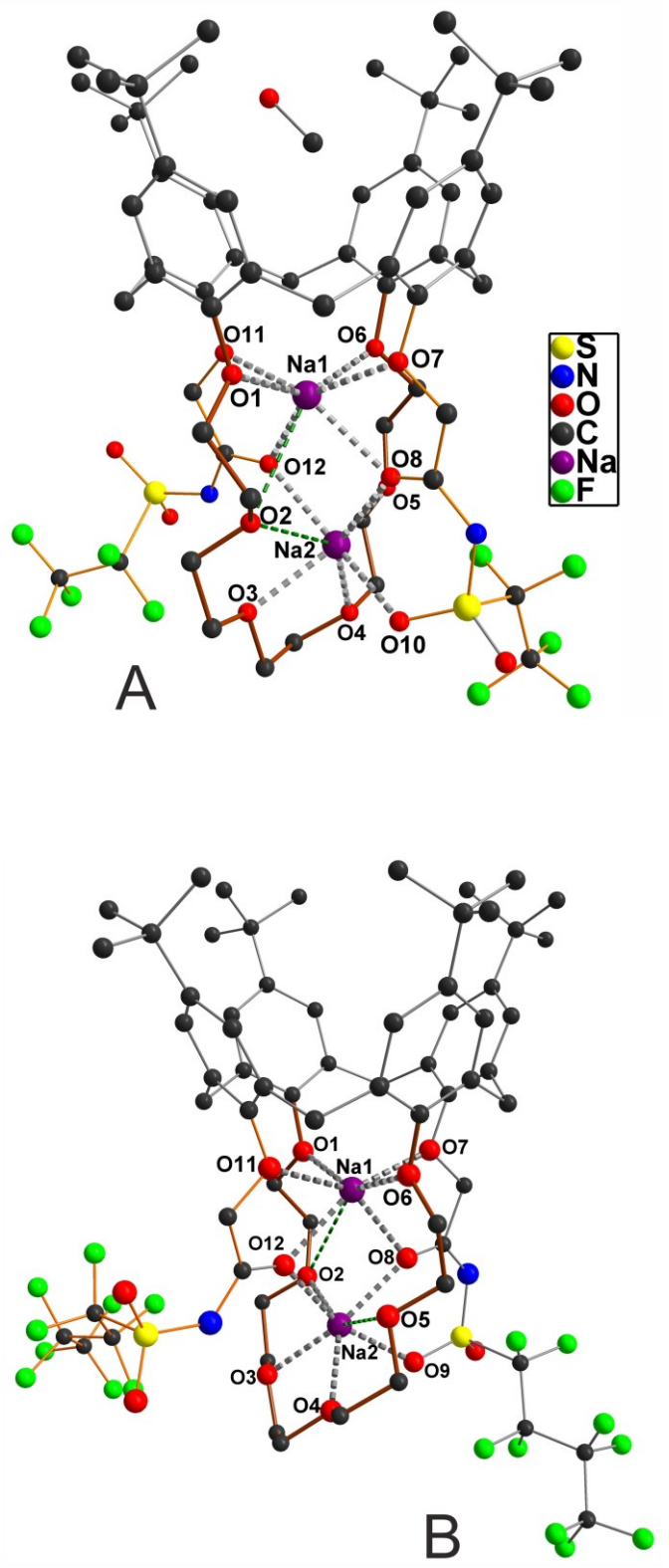


**Figure 1.** Molecular structures of the disodium complexes **Na8b** (**A**) and **Na8d** (**B**) in crystals of the respective compounds. The coordinative bonds are shown as thick, gray, dashed lines and the non-coordinating Na···O contacts as thin, green, dashed lines. Only one orientation of the disordered parts is shown for visibility reasons. Also, the hydrogen atoms and the co-crystallized solvents molecules with the only exception of the methanol molecules inside of the cage of **Na8b** (**A**) are omitted for better visibility.

distance in **8b** is found at 4.5 Å. In these expanded crown ether units two $Na^+$ cations can be incorporated, such that the $Na^+\cdots Na^+$ distances are out of the range of strong repulsive forces, i.e. 3.322(1) Å in **Na8b** and 3.403(1) Å in **Na8d**.In both compounds the sodium cations are coordinated by 6 oxygen atoms. The atom Na1 is coordinated by two oxygen atoms from the crown ether ring and four of the alkylsulfonamide chains, whereas Na2 is bonded to three oxygen atoms of the crown ether ring and three of the chains. In **Na8b** the Na···O distances are in the range of 2.236(1) Å to 2.596(2) Å. In **Na8d** the range from 2.247(2) Å to 2.431 Å is smaller (coordinative bonds are shown as thick dashed gray lines in Figure 1.). Beyond 3.0 Å, each of the Na atoms in **Na8b** and **Na8d** has one more contact to an oxygen atom of the crown ether bridge (shown as thin dashed green lines in Figure 1), but with significantly longer distances than the other six, i.e., Na1···O2 with 2.970(2) Å and Na2···O2 with 2.819(2) Å. They are shown in Figure 1A as dashed lines. The coordination environment of the $Na^+$ cations can be described as severely distorted octahedral, with O–Na–O angles of opposite oxygen atoms deviating from 180° by up to 49° (O3–Na2–O5). The coordination environment of both $Na^+$ ions is edge-sharing bi-octahedral.

The four phenyl groups of both compounds connected via $CH_2$-groups are tilted, such that the formed cages open up towards the outside. The respective opposite phenyl rings have an opening angle of the mean planes through the phenyl carbon atoms of 44.1° and 52.0° in **Na8b** as well as 40.1° and 53.1° in **Na8d**.

Beside the coordinated sodium, the crystals of **Na8b** and **Na8d** contain co-crystallised solvent molecules. A total of 3.64 methanol molecules per formula unit (sites not fully occupied) exist in **Na8b**, in which one is located inside of the cavity of the phenyl rings as shown in Figure 1A. Calix **Na8d** contains 1.74 molecules of toluene (not shown in Fig. 1B) per formula unit of calixarene.

The presence of $Na^+$ in the sodium complexes was further evidenced by $^{23}Na$ NMR (monoisotopic nucleus, spin 3/2). A standard solution of $NaClO_4$ was prepared in acetonitrile-$d_3$ and measured beforehand showing a narrow signal with a chemical shift at -2.8 ppm. In contrast, a broadened signal was detected

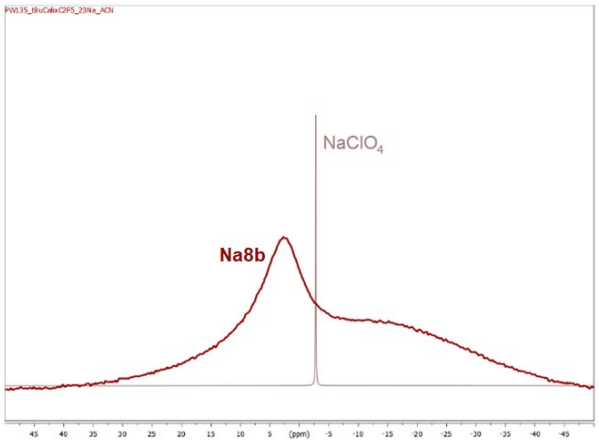


**Figure 2.** $^{23}Na$ NMR spectra of a $NaClO_4$ solution (gray) and calix-complex **Na8b** (red) both measured in acetonitrile-$d_3$.

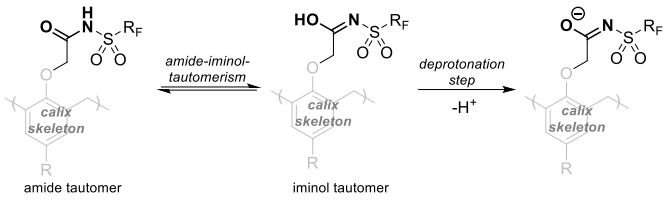


**Scheme 2.** Description of the amide-iminol-tautomerism followed by deprotonation of the highly acidic hydroxy group.

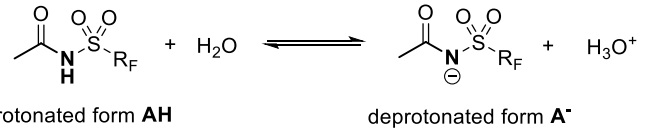


**Scheme 3.** Deprotonation reaction of the amide function of a mixed acetamide fragment **AH**/**A**$^-$.

for the complexes (e.g., δ = 2.7 ppm for **Na8b**, see Figure 2) coming from the unsymmetrical environment around the sodium ions due to the quadrupolar behavior.[45] Unfortunately, a distinction between the both complexed $Na^+$ ions in the calix complex was not possible, even after cooling.

**Tautomerism and acidity of the amide functions**

Interestingly, the metal ions $Na^+$ and $Ba^{2+}$ are bound via the oxygen atoms and not via the nitrogen atoms of the both carboxamide moieties as demonstrated recently by calculations[31] and as shown in the X-ray structures in Figures 1 and 4. The formation of the inimol tautomer according to the amide-iminol-tautomerism as step 1 in Scheme 2 is necessary for the formation of the complexes. We aimed at comparing the free energies of the two forms using the same computational setting (see Experimental Section) as for the $pK_a$ calculations. The reaction free energy is 9 kcal/mol, which demonstrates that the proton bound to the nitrogen atom (amide form) is thermodynamically favoured compared to the proton bound to the oxygen atom (iminol form).

The question regarding the acidity of the amide group that is attached to the lower rim of the calixcrowns was explored more detailed. In addition, the effect of different perfluorocarbon groups on the deprotonation of NH group was studied. To simplify the problem, the calculations were carried out on a fragment shown in Scheme 3. The free energies $\Delta G_{diss}$ and the corresponding $pK_a$ values calculated using the COSMO-RS solvation model (see the computational details) are presented in Table 1.

The free energy $\Delta G_{diss}$ representing the reaction energy of the dissociation reaction where **AH** and **A**$^-$ in Scheme 3 are the protonated and deprotonated forms, respectively, of the acid and $R_F$ = $CF_3$, $C_2F_5$, $C_3F_7$, $C_4F_9$, t-$C_4F_9$ is calculated according to equation:

$$\Delta G_{diss} = [G(A^-) + G(H_3O^+)] - [G(AH) + G(H_2O)]$$

The $pK_a$ values were calculated according to the expression:

$$pK_a = A\frac{\Delta G_{diss}}{RTln(10)} + B$$

where R is the ideal gas constant and T = 298 K. A and B are fitting constants calculated from the linear regression using the plot of $\Delta G_{diss}$ against the experimental $pK_a$ (for more details, see computationally methodology section).

**Table 1.** Dissociation free energy $\Delta G_{diss}$ and $pK_a$ values for the amide fragment (B3LYP-D3/def2-TZVP).

| $R_F$ | $\Delta G_{diss}$ (kcal/mol) | $pK_a$ |
|---|---|---|
| **$CF_3$** | 7.71 | 3.29 |
| **$C_2F_5$** | 7.73 | 3.30 |
| **i-$C_3F_7$** | 8.31 | 3.49 |
| **n-$C_4F_9$** | 6.24 | 2.79 |
| **t-$C_4F_9$** | 5.76 | 2.63 |

The calculated values follow the trend t-$C_4F_9$ = n-$C_4F_9$ < $CF_3$ = $C_2F_5$ < i-$C_3F_7$ where the least acidic group is i-$C_3F_7$ consistent with experimental findings.

**Preparation of the metal ion-free ligands**

Sodium-free calix ligands would be of favor, because the respective radionuclide $^{133}Ba$ or $^{224}Ra$ are in deficit stochiometric amounts compared to the amount of the ligands that may influence the radiolabeling behavior and could be problematic. To compare and overcome negative results, the respective sodium-free calixarenes **L7a-d** and **L8a-d** were prepared. For this purpose, the respective sodium complexes **Na7a-d** and **Na8a-d** were dissolved in dichloromethane or chloroform and the resulting solutions were washed with 10% aqueous HCl to force protonation of the amide side chains, which leads to the protonation of the calix and the dissociation of the Na-complex by pushing the $Na^+$ into the aqueous phase (Scheme 4). After separation of the organic layer, the solvent was removed to obtain the ligands **L7a-d** and **L8a-d** in quantitative yield. $^1H$, $^{13}C$ and $^{23}Na$ NMR spectra (Figures 2 and 3) were recorded to prove the absence of $Na^+$. The absence of the signal in the $^{23}Na$ NMR spectra and changes of the chemical shifts in the $^1H$ NMR spectra clearly showed the existence of a new species, which was identified as free ligands **L7a-d** and **L8a-d**. Additionally, signals for the NH function at a chemical shift between 10 and 11 ppm of the sulfonamide moiety were found, indicating the existence of the amide tautomer. Based on calculations, the chemical shift of the iminol OH proton is more downfield shifted.[46]

**Investigation of the barium complexes**

To reach our central aim to prepare radium complexes with functionalized calix[4]arene ligands, $Ba^{2+}$ was used as nonradioactive surrogate to create the reference complexes. The desired Ba-complexes **Ba7a-d** and **Ba8a-d** were yielded quantitatively after dissolving the sodium-free ligands **L7a,b,d**

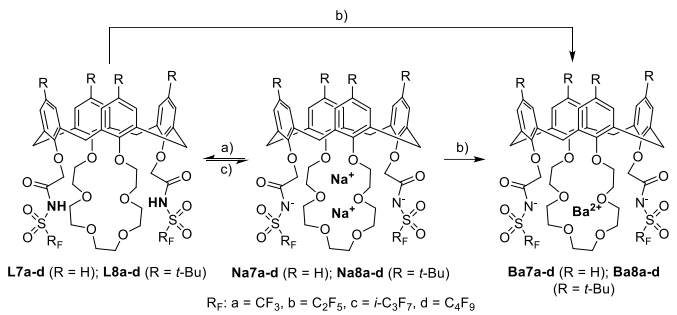


**Scheme 4.** Preparation of the ion-free ligands **L7a,b,d, L8a-d** and the respective barium complexes **Ba7a-d, Ba8a-d**. *Reagents and conditions:* a) 10% aqueous HCl; b) $Ba(ClO_4)_2$, acetonitrile, ultrasound, 5 min; c) $NaClO_4$, acetonitrile, ultrasound, 5 min.

and **L8a-d** in acetonitrile with an excess of 5 equiv. of $Ba(ClO_4)_2$. After treatment with ultrasound for 5 min, the solvent was removed and dichloromethane or chloroform was added to the residue. Since all resulting Ba-complexes **Ba7a-d** and **Ba8a-d** were again obtained as neutral complexes, they are soluble in the organic solvent and remained in solution, whereas $Ba(ClO_4)_2$ was insoluble and could be removed by filtration. The filtrate contained solely the pure barium complexes after final removal of the solvent.

To additionally prove the chelation behavior of the Na-complexes **Na7a-d** and **8a-d** in the presence of $Ba(ClO_4)_2$, the same procedure as described before was accomplished. Interestingly, both $Na^+$ cations were completely removed from the calix[4] scaffold and exchanged with $Ba^{2+}$. The desired Ba-complexes **Ba7a-d** and **Ba8a-d** were obtained in quantitative yields. The whole complexation procedure including the central ion exchange is presented in Scheme 4. This prompted us to accomplish reactions using both the Na-complexes **Na7a-d** and **Na8a-d** as well as the Na-free ligands **L7a,b,d** and **L8a-d** for further complexation with $Ba^{2+}$ and for the radiolabeling procedures with $^{133}Ba$ and $^{224}Ra$. The existence of the Ba-complexes **Ba7a-d** and **Ba8a-d** was verified by $^1H$ and $^{13}C$ NMR spectroscopy. Distinct changes of the chemical shifts were observed between the Na-complexes, the free ligands and the Ba-complexes as seen for instance in the $^1H$ NMR spectra of **L8d**, **Na8d**, and **Ba8d** in Figure 3 and Table 2.

The influence of the metal ion ($Na^+$ vs. $Ba^{2+}$) on the crown bridge and the calix-skeleton in comparison to the free ligand is nicely to determine from the $^1H$ NMR analyses and will be discussed exemplarily. All signals from the crown are well separated and occur at different chemical shifts for the both complexes **Na8d** and **Ba8d** in contrast to the free ligand **L8d**. There, the signals are broadened and overlap due to the higher flexibility of the calix-crown. Furthermore, the signals of the *tert*-butyl groups of the Na-complex are close together ($\Delta\delta$ = 0.04 ppm) in high contrast to the free ligand ($\Delta\delta$ = 0.52 ppm) and the Ba-complex ($\Delta\delta$ = 0.35 ppm). The same phenomenon was found for the signals in the aromatic region (Table 1).

However, NMR-based titrations with the ligands and $Ba^{2+}$ are not appropriate to determine association constants due to the slow metal exchange with regard to the NMR time scale (see Figures 67 and 68 of the Supporting Information, e.g., for **Na7a**).

Two separate species **Na7a** and **Ba7a** occurred in the $^1H$ NMR as well as in the $^{19}F$ NMR spectra during the addition of $Ba^{2+}$. After the addition of 1 eq. of $Ba(ClO_4)_2$, no ligand was detectable anymore, which leads to the assumption of a complex with 1:1 stoichiometry.

**Table 2.** Selected chemical shifts from the $^1H$ NMR analyses of the free ligand **L8d**, the sodium-complex **Na8d**, and the barium-complex **Ba8d** measured in $CDCl_3$.

| Assignment | free ligand L8d/ppm | Na-complex Na8d/ppm | Ba-complex Ba8d/ppm |
|---|---|---|---|
| $^t$Bu | 0.81 / 1.33 | 1.10 / 1.14 | 0.93 / 1.28 |
| $CH_{2,\ endo}$ | 3.25 | 3.37 | 3.32 |
| $CH_{2,\ exo}$ | 4.54 | 4.14 | 4.31 |
| $CH_2C{=}O$ | 5.26 | 4.62 | 4.47 |
| Ar-H | 6.46 / 7.10 | 7.07 / 7.10 | 6.85 / 7.21 |

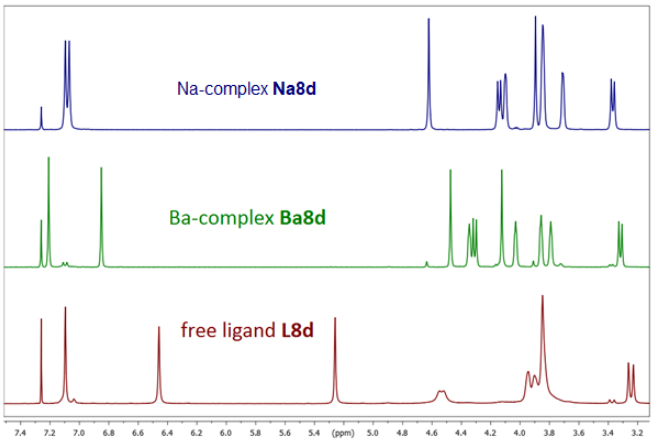


**Figure 3.** Comparison of $^1H$ NMR spectra (region of interest: 3.0-7.5 ppm) from free ligand **L8d**, disodium complex **Na8d** and barium complex **Ba8d** measured in $CDCl_3$.

Single crystals of the barium-complex **Ba8d** were obtained suitable for an X-ray structure analysis. The molecular structure is shown in Figure 4. A tenfold oxygen coordination is found for the central barium ion in **Ba8d**. It is located in the centre of the crown ether moiety, being coordinated to all six oxygen atoms O1 to O6 of the ring. The distances of these coordinative bonds range from 2.807(2) Å to 2.946(3) Å. Each perfluorinated alkylsulfonamide chain contributes two more coordinating oxygen atoms in a distance range from 2.703(2) Å to 3.036(2) Å. This is in good accordance to the calculated optimized geometry (Figure 50 and Table S1 of the SI). The much larger ionic radius of $Ba^{2+}$ (Shannon radius 1.52 Å, 10fold coordination) compared to $Na^+$ (1.02 Å, six-fold coordination) leads to the fact that two $Na^+$ ions with CN = 6 are present in **Na8b** and **Na8d**, whereas one $Ba^{2+}$ ion is 10-fold coordinated in **Ba8d**.[47] Similar to those of **Na8b** and **Na8d**, crystals of **Ba8d** contain co-crystallised solvent molecules, in this case three chloroform molecules per formula unit. One of these as well as two of the *tert*-butyl groups are disordered, what has been treated using split models in the structure refinement.

**Validation of the association constants for $Ba^{2+}$ and $Ra^{2+}$**

A reliable method to determine stability constants of $M^{2+}$-calixarene-complexes *via* UV-Vis spectroscopy was developed in the past.[28,31] However, this method is carried out at its limit of validation for these functionalized calix-crowns,[48] so that

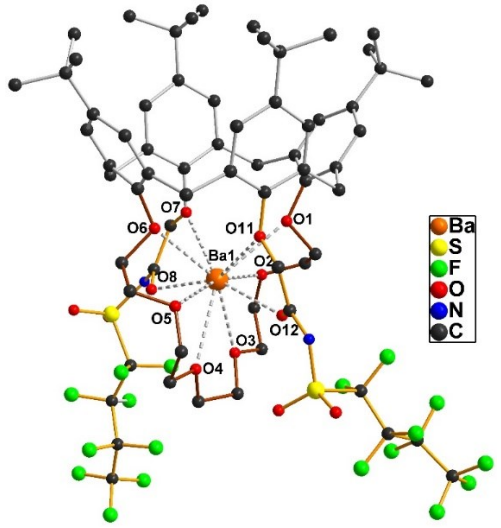


**Figure 4.** Molecular structure of the barium complex **Ba8d** in the crystal without the co-crystallized $CHCl_3$ molecules. Only one of the two disordered orientations of the $^t$Bu groups is shown for better visibility.

values greater than 5 are associated with a large error.[49,50] Furthermore, the UV-Vis method is not appropriate for $Ra^{2+}$, since a high amount of the metal salt would be required. Due to these limits, a novel radiochemical two-phase-extraction method, using the radionuclides Ba-133 and Ra-224, was established. The experiments were performed with aqueous solutions of barium-133 as $[^{133}Ba]BaCl_2$ (half-life: 10.5 a, carrier added) and radium-224 as $[^{224}Ra]Ra(NO_3)_2$ (3.6 d, no-carrier-added). The functionalized calixarenes as free ligands **L7a-d** and **L8a-d** as well as two of the $Na^+$-complexes **Na7a** and **Na8a** (for comparison of the free ligand and the sodium complex) were analyzed at a pH of 6. For these experiments, an excess (approx. 10- to 1000-fold) of each ligand over the radiometal ion was used. The radioactivity count rates of the radiometal which was extracted to the ligand-containing chloroform phase ($M^{2+}$-calix-complex) as well as the remaining radioactivity in the aqueous phase (unbound $M^{2+}$) were determined as average values out of three experiments. All data of the radium experiments were obtained after 4 days to ensure the total decay of initial $^{212}$Pb which was extracted as well. The results in Table 3 are expressed as calculated log*K* values for the respective calixarene-metal-complexes in chloroform out of the radioactivity distribution equilibrium. The calculation was performed according to Haupt and co-workers.[51]

The association constants of the sodium complexes **Na7a** and **Na8a** are slightly higher compared to the free ligands **L7a-d** and **L8a-d**. This effect might be due to the different energy amounts which are needed for the H→Ba(Ra) and the Na→Ba(Ra) exchange to form the respective complex. Consequently, we decided to perform all further experiments only with the sodium-free ligands. Moreover, it is shown, that the ligands **L7a-d** (R = H) form complexes with significantly lower log*K* values in chloroform compared to ligands **L8a-d** (R = $^t$Bu) due to the different flexibility of the calix-skeleton combined with the influence for the crown. All ligands were initially tested at a concentration of $10^{-3}$ M. When a complete extraction of the

**Table 3.** Experimental logK values from extraction procedure with $[^{133}Ba]Ba^{2+}$ and $[^{224}Ra]Ra^{2+}$.

| Calix | R | $R_F$ | $c_{calix}$ [M] | logK (Ba) | logK (Ra) |
|---|---|---|---|---|---|
| **Na7a** | H | $CF_3$ | $10^{-3}$ | 5.3±0.1 | 5.6±0.1 |
| **Na8a** | $^t$Bu | $CF_3$ | $10^{-3}$ | 6.3±0.1 | 5.6±0.1 |
| **L7a** | H | $CF_3$ | $10^{-3}$ | 4.2±0.1 | 4.1±0.1 |
| **L7b** | H | $C_2F_5$ | $10^{-3}$ | 4.8±0.1 | 4.3±0.1 |
| **L7c** | H | i-$C_3F_7$ | $10^{-3}$ | 5.5±0.1 | 4.5±0.1 |
| **L7c** | H | i-$C_3F_7$ | $10^{-4}$ | 6.7±0.1 | n.d. |
| **L7c** | H | i-$C_3F_7$ | $10^{-5}$ | 7.5±0.1 | n.d. |
| **L7d** | H | $C_4F_9$ | $10^{-5}$ | 5.0±0.1 | 5.8±0.1 |
| **L8a** | $^t$Bu | $CF_3$ | $10^{-3}$ | 5.6±0.1 | 4.5±0.1 |
| **L8b** | $^t$Bu | $C_2F_5$ | $10^{-3}$ | 6.0±0.1 | 4.7±0.1 |
| **L8c** | $^t$Bu | i-$C_3F_7$ | $10^{-3}$ | 6.6±0.1 | 5.2±0.1 |
| **L8c** | $^t$Bu | i-$C_3F_7$ | $10^{-4}$ | 7.8±0.1 | n.d. |
| **L8c** | $^t$Bu | i-$C_3F_7$ | $10^{-5}$ | 8.2±0.1 | n.d. |

radioactivity from the aqueous to the organic phase was detected, lower ligand concentrations of $10^{-4}$ M and $10^{-5}$ M were tested as well, especially regarding the ligands **L7c/d** and **L8c/d**. Comparing the perfluorinated side chains, a tendency of the log*K* values was found to be $CF_3 < C_2F_5 <$ i-$C_3F_7 > C_4F_9$, which is in good accordance to the DFT calculations. The highest association constant for a barium complex was found for the $^t$Bu-bearing **L8c** with a logK of 8.2.

Stability and selectivity of the calixarene complexes were further characterized by using the calix complexes **Ba7a-d** and **Ba8a-d** as well as **Ra7a-d** and **Ra8a-d** in chloroform and a second extraction step with $Ca^{2+}$ as a physiologically competing alkaline earth metal cation. For this purpose, an isotonic $CaCl_2$ solution (1%) was used and the chloroform solution containing the calix complexes **Ba7a-d** and **Ba8a-d** as well as **Ra7a-d** and **Ra8a-d** were extracted again for one hour at room temperature. Afterwards, the radioactivity distribution between the aqueous and the chloroform phase was determined. The Ba-complexes showed a small release of activity between 1% and 3% within one hour of incubation. Furthermore, a slightly higher release of 6-8% was observed for the respective radium-complexes in the same time frame. It has to be considered that the radium release occurred mainly from the daughters $^{212}$Pb and $^{212}$Bi as part decay product of $^{220}$Rn which is the first decay product of the α-decay chain of $^{224}$Ra and easily diffuses from one phase to another. Thus, the stability of the complexes regarding the direct radium release is significantly higher. To conclude, all tested complexes show relevant stability against calcium ions in 40-fold excess (to ligand) as well as selectivity for barium und radium over calcium. Therefore, barium- and radium-calixarene complexes with perfluorinated side chains could be suitable chelators providing acceptable complex stabilities and low ratios of decomplexation under *in vivo* conditions. All results

regarding the metal release of the complexes are summarized in Table 4.

**Table 4.** Stability testing of the calix-complexes with 1% aqueous $Ca^{2+}$ solution.

| Calix | R | $R_F$ | % release from $^{133}$Ba-complex | % release from $^{224}$Ra-complex* |
|---|---|---|---|---|
| **7a** | H | $CF_3$ | 3 | 7 |
| **7b** | H | $C_2F_5$ | 2 | 7 |
| **7c** | H | i-$C_3F_7$ | 1 | 7 |
| **7d** | H | $C_4F_9$ | 3 | 6 |
| **8a** | $^t$Bu | $CF_3$ | 1 | 8 |
| **8b** | $^t$Bu | $C_2F_5$ | 1 | 8 |
| **8c** | $^t$Bu | i-$C_3F_7$ | 1 | 8 |

* mainly the daughters $^{212}$Pb and $^{212}$Bi from α-decay chain of $^{224}$Ra.

**Table 5.** Binding energies of calix[4]crown-6 complexes with $R_F = CF_3$ at the side chain and R = H (**Ba7a** and **Ra7a**) and $^t$Bu (**Ba8a** and **Ra8a**) at the upper rim complexing different metal ions calculated using B3LYP-D3/def2-TZVP (E is electronic energy).

| Complex | R | $R_F$ | ΔE (kcal/mol) |
|---|---|---|---|
| **Ba7a** | H | $CF_3$ | -97.32 |
| **Ba8a** | $^t$Bu | $CF_3$ | -100.90 |
| **Ra7a** | H | $CF_3$ | -98.82 |
| **Ra8a** | $^t$Bu | $CF_3$ | -102.78 |

### Comparison between $Ba^{2+}$ and $Ra^{2+}$ binding and the effect of the substitution on the upper rim

We have conducted computational studies using Kohn-Sham density functional theory (DFT) to compare the binding affinity of $Ba^{2+}$ and $Ra^{2+}$ ions toward the calixcrowns. The computational analysis aimed towards answering two important questions: The first one regarding the binding preference of the two metal ions to the calix[4]crown-6 and the second one concerning the effect of substituting the H by $^t$Bu groups on the upper rim of the calixarene on the host-guest-interaction. The numbers shown in Table 5 represent the binding strength of the metal ions to the pre-organized geometry (the metal free equilibrium geometry of the complex). With our computational settings, we have found that $Ra^{2+}$ complexes are slightly more stable by around 1.5 kcal/mol compared to the $Ba^{2+}$ containing molecules. Regarding the *tert*-butyl substitution, the binding energies for both complexes (Ra and Ba) are more negative by around 3.5 kcal/mol for the butylated upper rim complex.

## Experimental

### General

All chemicals were purchased from commercial suppliers and used without further purification unless otherwise specified. Anhydrous THF was purchased from Acros or Sigma-Aldrich, anhydrous $Ba(ClO_4)_2$ was purchased from Alfa Aesar and deuterated solvents were purchased from deutero GmbH. Compounds **2, 4, 6,** and **Na8a** were prepared according to ref. 28, compound **1** according to refs. 29 and 30, compounds **3** and **5** according to ref. 43 and compound **Na8c** according to ref. 31. Heptafluoropropane-2-sulfonamide was synthesized according to a procedure published by Steibeisser et al.[52] [$^{133}$Ba]$BaCl_2$ (carrier added) was purchased from Polatom. NMR spectra of all compounds were recorded on an Agilent DD2-400 MHz NMR or an Agilent DD2-600 MHz NMR spectrometer with ProbeOne. Chemical shifts of the $^1$H, $^{19}$F, and $^{13}$C spectra were reported in parts per million (ppm) using TMS as internal standard for $^1$H/$^{13}$C and $CFCl_3$ for $^{19}$F spectra. Mass spectrometric (MS) data were obtained on a Xevo TQ-S mass spectrometer (Waters) by electron spray ionization (ESI). The melting points were determined on a Galen III melting point apparatus (Cambridge Instruments & Leica) and are uncorrected. TLC detections were performed using Merck Silica Gel 60 F254 sheets. TLCs were developed by visualization under UV light (λ = 254 nm). Chromatographic separations were accomplished by using an automated silica gel column chromatography system Biotage Isolera Four and appropriate Biotage KP-SIL SNAP columns. Diffraction data was collected with a Bruker Apex Kappa-II CCD diffractometer using graphite-monochromated Mo-Kα radiation (λ = 0.71073 Å) and the measurement was performed at −150 °C. The structure was solved by direct methods and refined against $F^2$ by full-matrix least-squares using the program suites from G. M. Sheldrick.[54-56] All non-hydrogen atoms were refined anisotropically; all hydrogen atoms were placed on geometrically calculated positions and refined using a riding model. In the structure of the calix **Na8b**, one of the four *tert*-butyl groups and one of the two $SO_2C_2F_5$ groups are disordered. The disordered groups were refined by split models with the sum of the occupational factors of the two split arrangements being fixed to unity. The same holds for one of the four $^t$Bu-phenyl units in the structure of **Na8d**. Only one of each disordered orientation is shown in Figure 1. CCDC-1950767 (**Na8b**), CCDC-1950687 (**Na8d**), and CCDC-1912291 (**Ba8d**) contain the supplementary crystallographic data. These data can be obtained free of charge from The Cambridge Crystallographic Data Centre via http://www.ccdc.cam.ac.uk/data_request/cif.

### Liquid/liquid extraction method with $^{133}$Ba and $^{224}$Ra

Thorium-228 as source for [$^{224}$Ra]$Ra^{2+}$ was obtained from Eckert & Ziegler. Radium-224 was isolated from this $^{228}$Th-source as [$^{224}$Ra]$Ra(NO_3)_2$ in 1.0 M HCl using ion exchange and extractive chromatography methods from thorium-228 as reported previously.[53] For any of the liquid/liquid extraction experiments, the respective ligand was dissolved in 600 µL chloroform in a certain final concentration ($10^{-3}$ M - $10^{-5}$ M). The radionuclide ($^{224}$Ra or $^{133}$Ba, respectively; approx. 50-100 kBq) was diluted to a total volume of 600 µL with deionized $H_2O$ and the pH was adjusted to 6. After shaking the samples at room temperature for 1 hour, 200 µL of each phase were taken out for analyzing the radioactivity count rates. Count rates were recorded by the sodium iodide crysral gamma spectrometer ISOMED 2160. The distribution equilibrium was finally transferred into the following equation, which was used for log*K* calculation:

$$logK = log\left(\frac{1}{c_{Lig}} \cdot \frac{cpm_{org}}{cpm_{aq}}\right)$$

With $c_{Lig}$ being the ligand concentration and $cpm_{org/aq}$ the recorded radioactive count rates in the queous/organic phase. The method was followed according the published procedure by Haupt et al.[51]

**The computational methodology**

The calculations of calixcrowns were performed using Kohn-Sham DFT. The general gradient approximation (GGA) functional BP86[57,58] was used for geometry optimizations presented in the Results and Discussion Section. The well-known hybrid Becke's functional B3LYP[59,60] was chosen to perform single point energy calculations. With the latter settings, we have used a continuum solvation model COSMO for acetonitrile (dielectric constant $\zeta = 37.5$) in order to approximately include the solvent environment used in the experiment. Ahlrichs' triple zeta valence polarized (def2-TZVP) [61] basis set was employed as well as the resolution of identity approach and corresponding auxiliary basis sets,[62] along with Grimme's D3 dispersion correction.[63] Since the def2-TZVP has not been available for radium yet, we have used the split valence polarized (def-SVP) basis set[64] for both $Ra^{2+}$ and $Ba^{2+}$ in the calculations that involved a comparison between their binding energies. Turbomole 7.3 package[65] was used for all calculations in this study. To prevent the over-stabilization of reaction energies, basis set superposition error was considered. Due to the smaller molecular size, the calculations for the fragment used to calculate the acidity and tautomerism were carried out using B3LYP and def2-TZVP. The free energies were calculated by adding corrections regarding the entropy and zero-point energies. In order to achieve reasonable prediction of $pK_a$ values, we have applied the solvation continuum model COSMO for more realistic solvation (COSMO-RS) to the conductor limit ($\zeta = \infty$) as implemented in Turbomole and described in Ref. 66. The molecules are: boric acid, 2,2,2-trichloroethanol, uracil, 3,5-dichlorophenol, sulfurous acid, chloroacetic acid, carbonic acid, valeric acid, tert-butyl alcohol, succinimide, bromoacetic acid, iodoacetic acid, methanol, 4-chlorophenol, dichloroacetic acid, benzoic acid, ethanol, fumaric acid, cyanoacetic acid, fluoroacetic acid, phenol, trichloroacetic acid, nitrous acid, acetic acid, formic acid, 2,2-dimethylpropionic acid, 2-hydroxypropionic acid, acrylic acid, maleic acid, oxalic acid, phthalic acid, thymine, trans-5-formyl uracil, 3,3-dimethylsuccinimide, 3-methyl-3-phenylglutarimide, $H_2O$.

**General procedure for the synthesis of the Na-complexes Na7a-d and Na8a-d**

25,27-Bis(carboxymethoxy)-calix[4]aren-crown-6 (**5**) or 5,11,17,23-tetra-*tert*-butyl-25,27-bis(carboxymethoxy)-calix[4]aren-crown-6 (**6**) (1 equiv.) was suspended in anhydrous $CCl_4$ (5 mL). Oxalyl chloride (min. 10 equiv.) was added and the mixture was stirred for 5 h at 65°C. After cooling to rt, the solvent and remaining oxalyl chloride was removed. Under argon, the residue was dissolved in anhydrous dichloromethane (5 mL) and a mixture of the respective perfluoralkyled sulfonamide (2.2-2.5 equiv.) and NaH (60% in mineral oil, 10 equiv.) dissolved in anhydrous dichloromethane added. After stirring overnight at rt, the mixture was filtered, the organic phase was washed with 10% HCl, the organic phase was separated and dried over $Na_2SO_4$. Next, the solvent was removed and the crude product was purified by (automated) column chromatography (solvent: dichloromethane → dichloromethane/methanol 5:1) to yield the calixarenes **Na7a-d** and **Na8a-d** as colorless solids.

**Disodium 25,27-bis(*N*-trifluoromethanesulfonylcarbamoylmethoxy)calix[4]arene-crown-6 (Na7a)**

Compound **5** (810 mg, 1.09 mmol), oxalyl chloride (5.5 mL), NaH (440 mg, 11 mmol) and trifluoromethanesulfonamide (370 mg, 2.41 mmol) were reacted according to the general synthesis procedure to yield 490 mg (45%) of **7a**. M.p. >310°C (decomp); $^1$H NMR (600 MHz, $CDCl_3$): δ = 3.45 (d, $^2J$ = 12.5 Hz, 4H, $ArCH_2$), 3.73–3.78 (m, 4H, $OCH_2$), 3.85–3.91 (m, 8H, $OCH_2$), 3.93 (s, 4H, $OCH_2$), 4.11–4.16 (m, 4H, $OCH_2$), 4.22 (d, $^2J$ = 12.5 Hz, 4H, $ArCH_2$), 4.65 (s, 4H, $CH_2C$=O), 6.82–6.92 (m, 4H, ArH), 7.10–7.17 (m, 8H, ArH). $^{13}$C NMR (101 MHz, $CDCl_3$): δ = 29.9 ($ArCH_2$), 69.4, 69.5, 72.0, 72.1 (4 x $OCH_2$), 77.2 ($\underline{C}H_2C$=O), 79.3 ($OCH_2$), 120.5 (q, $^1J_{C,F}$ = 322 Hz, $CF_3$), 126.1, 126.6 (2 x *p*-$C_{Ar}$), 129.3, 129.7 (2 x *m*-$C_{Ar}$), 134.8, 135.0 (2 x *o*-$C_{Ar}$), 150.9, 154.0 (2 x *i*-$C_{Ar}$), 175.8 (C=O). $^{19}$F NMR (376 MHz, $CDCl_3$): δ = −79.3 ($CF_3$). MS (ESI+): *m/z* (%) = 1005 (53) [M – 2Na$^+$ + H$^+$], 1027 (100) [M – Na$^+$].

**Disodium 25,27-bis(*N*-pentafluoroethanesulfonylcarbamoylmethoxy)calix[4]arene-crown-6 (Na7b)**

Compound **5** (300 mg, 0.40 mmol), oxalyl chloride (1.5 mL), NaH (162 mg, 4.03 mmol) and pentafluoroethanesulfonamide (201 mg, 1.00 mmol) were reacted according to the general synthesis procedure to yield 213 mg (47%) of **7b**. $^1$H NMR (600 MHz, $CDCl_3$): δ = 3.45 (d, $^2J$ = 12.5 Hz, 4H, $ArCH_2$), 3.75 (br. s, 4H, $OCH_2$), 3.84-3.95 (m, 12 H, 3 x $OCH_2$), 4.14 (br. s, 4H, $OCH_2$), 4.22 (d, $^2J$ = 12.5 Hz, 4H, $ArCH_2$), 4.65 (s, 4H, $CH_2C$=O), 6.82-6.92 (m, 4H, *p*-$H_{Ar}$), 7.09-7.16 (m, 8H, *m*-$H_{Ar}$). $^{13}$C NMR (151 MHz, $CDCl_3$): δ = 29.9 ($ArCH_2$), 69.4, 69.5, 72.1, 72.2, (4 x $OCH_2$), 77.2 ($\underline{C}H_2C$=O), 78.9 ($OCH_2$), 126.1, 126.5 (2 x *p*-$C_{Ar}$), 129.3, 129.7 (2 x *m*-$C_{Ar}$), 134.7, 135.0 (2 x *o*-$C_{Ar}$), 150.9, 154.0 (2 x *i*-$C_{Ar}$), 176.0 (C=O). $^{19}$F NMR (565 MHz, $CDCl_3$): δ = -117.9 (4F), -78.9 (6F). MS (ESI+): *m/z* (%) = 1181 (26) [M – 2Na$^+$ + H$^+$], 1203 (88) [M – Na$^+$].

**Disodium 25,27-bis(*N*-heptafluoropropane-2-sulfonylcarbamoylmethoxy)calix[4]arene-crown-6 (Na7c) H-$C_3F_7$**

Compound **5** (300 mg, 0.40 mmol), oxalyl chloride (1.5 mL), NaH (162 mg, 4.03 mmol) and perfluoroisopropanesulfonamide (252 mg, 1.00 mmol) were reacted according to the general synthesis procedure to yield 195 mg (40%) of **7c**. $^1$H NMR (600 MHz, $CDCl_3$): δ = 3.45 (d, $^2J$ = 12.4 Hz, 4H, $ArCH_2$), 3.74 (br. s, 4H, $OCH_2$), 3.85 (br. s, 4H, $OCH_2$), 3.88-3.93 (m, 8 H, 2 x $OCH_2$), 4.14 (br. s, 4H, $OCH_2$), 4.21 (d, $^2J$ = 12.4 Hz, 4H, $ArCH_2$), 4.64 (s, 4H, $CH_2C$=O), 6.83-6.92 (m, 4H, *p*-$H_{Ar}$), 7.10-7.16 (m, *m*-$H_{Ar}$). $^{13}$C NMR (151 MHz, $CDCl_3$): δ = 29.8 ($ArCH_2$), 69.4, 69.4, 72.1, 72.2, (4 x $OCH_2$), 77.2 ($\underline{C}H_2C$=O), 79.3 ($OCH_2$), 126.1, 126.6 (2 x *p*-$C_{Ar}$), 129.3, 129.7 (2 x *m*-$C_{Ar}$), 134.8, 135.0 (2 x *o*-$C_{Ar}$), 150.9, 154.0 (2 x *i*-$C_{Ar}$), 176.0 (C=O). $^{19}$F NMR (565 MHz, $CDCl_3$): δ = -169.3 (2F),

 

-71.7 (12F). MS (ESI+): *m/z* (%) = 1205 (67) [M – 2Na$^+$ + H$^+$], 1227 (100) [M – Na$^+$].

**Disodium 25,27-bis(*N*-nonafluoroethane-1-sulfonylcarbamoylmethoxy)calix[4]arene-crown-6 (Na7d)**

Compound **5** (314 mg, 0.42 mmol), oxalyl chloride (1.5 mL), NaH (169 mg, 4.23 mmol) and heptafluoroisopropanesulfonamide (316 mg, 1.06 mmol) were reacted according to the general synthesis procedure to yield 148 mg (26%) of **7d**. $^1$H NMR (600 MHz, $CDCl_3$): δ = 3.45 (d, $^2J$ = 12.4 Hz, 4H, $ArCH_2$), 3.74 (br. s, 4H, $OCH_2$), 3.83-3.94 (m, 12 H, 3 x $OCH_2$), 4.14 (br. s, 4H, $OCH_2$), 4.22 (d, $^2J$ = 12.4 Hz, 4H, $ArCH_2$), 4.66 (s, 4H, $CH_2C$=O), 6.83-6.92 (m, 4H, *p*-$H_{Ar}$), 7.10-7.17 (m, *m*-$H_{Ar}$). $^{13}$C NMR (151 MHz, $CDCl_3$): δ = 29.9 ($ArCH_2$), 69.3, 69.4, 71.8, 71.9, (4 x $OCH_2$), 77.2 ($\underline{C}H_2C$=O), 79.2 ($OCH_2$), 126.0, 126.4 (2 x *p*-$C_{Ar}$), 129.2, 129.6 (2 x *m*-$C_{Ar}$), 134.8, 135.1 (2 x *o*-$C_{Ar}$), 151.1, 154.0 (2 x *i*-$C_{Ar}$), 174.1 (C=O). $^{19}$F NMR (565 MHz, $CDCl_3$): δ = -125.9 (4F), -121.1 (4F), -113.8 (4F), -80.8 (6F). MS (ESI+): *m/z* (%) = 1259 (45) [M – 2Na$^+$ + H$^+$], 1281 (96) [M – Na$^+$].

**Disodium 5,11,17,23-tetrakis(*tert*-butyl)-25,27-bis(*N*-pentafluoroethanesulfonylcarbamoylmethoxy)calix[4]arene-crown-6 (Na8b)**

Compound **6** (300 mg, 0.31 mmol), oxalyl chloride (1.5 mL), NaH (124 mg, 3.1 mmol) and perfluoroethanesulfonamide (154 mg, 0.77 mmol) were reacted according to the general synthesis procedure to yield 207 mg (50%) of **8b**. $^1$H NMR (600 MHz, $CDCl_3$): δ = 1.11 (s, 18H, $CH_3$), 1.15 (s, 18H, $CH_3$), 3.38 (d, $^2J$ = 12.2 Hz, 4H, $ArCH_2$), 3.73 (br. s, 4H, $OCH_2$), 3.87 (s, 8H, $OCH_2$), 3.92 (s, 4H, $OCH_2$), 4.08-4.19 (m, 8H, $OCH_2$+$ArCH_2$), 4.63 (s, 4H, $CH_2C$=O), 7.08 (s, 4H, *m*-$H_{Ar}$), 7.11 (s, 4H, *m*-$H_{Ar}$). $^{13}$C NMR (151 MHz, $CDCl_3$): δ = 30.1 ($ArCH_2$), 31.3, 31.5 (2 x $CH_3$), 34.2, 34.4 ($C_q$), 69.3, 69,4, 72.0, 72.1, (4 x $OCH_2$), 77.0 ($\underline{C}H_2C$=O), 79.3 ($OCH_2$), 125.8, 126.3 (2 x *m*-$C_{Ar}$), 134.1, 134.4 (2 x *o*-$C_{Ar}$), 147.8, 148.5 (2 x *p*-$C_{Ar}$), 148.4, 151.4 (2 x *i*-$C_{Ar}$), 176.2 (C=O). $^{19}$F NMR (565 MHz, $CDCl_3$): δ = -117.9 (4F), -78.9 (6F). MS (ESI+): *m/z* (%) = 1329 (53) [M – 2Na$^+$ + H$^+$], 1351 (100) [M – Na$^+$].

**Disodium 5,11,17,23-tetrakis(*tert*-butyl)-25,27-bis(*N*-nonafluoroethane-1-sulfonylcarbamoylmethoxy)calix[4]arene-crown-6 (Na8d)**

Compound **6** (317 mg, 0.33 mmol), oxalyl chloride (1.5 mL), NaH (131 mg, 3.3 mmol) and perfluorobutanesulfonamide (216 mg, 0.72 mmol) were reacted according to the general synthesis procedure to yield 346 mg (69%) of **8d**. $^1$H NMR (600 MHz, $CDCl_3$): δ = 1.10 (s, 18H, $CH_3$), 1.14 (s, 18H, $CH_3$), 3.37 (d, $^2J$ = 12.3 Hz, 4H, $ArCH_2$), 3.71 (br. s, 4H, $OCH_2$), 3.85 (br. s, 8H, OCH2), 3.90 (s, 4H, $OCH_2$), 4.07-4.17 (m, 8H, $OCH_2$+$ArCH_2$), 4.62 (s, 4H, $CH_2C$=O), 7.07 (s, 4H, m-$H_{Ar}$), 7.10 (s, 4H, m-$H_{Ar}$). $^{13}$C NMR (151 MHz, $CDCl_3$): δ = 30.0 ($ArCH_2$), 31.3, 31.4 (2 x $CH_3$), 34.1, 34.3 ($C_q$), 69.3, 69.4, 72.0, 72.1, (4 x $OCH_2$), 77.0 ($\underline{C}H_2C$=O), 78.8 ($OCH_2$), 125.8, 126.2 (2 x *m*-$C_{Ar}$), 134.1, 134.3 (2 x *o*-$C_{Ar}$), 147.8, 148.3 (2 x *p*-$C_{Ar}$), 148.4, 151.4 (2 x *i*-$C_{Ar}$), 162.7 (C=O). $^{19}$F NMR (565 MHz, $CDCl_3$): δ = -126.0 (4F), -121.1 (4F), -113.8 (4F), -80.8 (6F). MS (ESI+): *m/z* (%) = 788 (51) [M/2 + 2H$^+$].

**Synthesis of the barium-complexes**

**General procedure**

The sodium complexes **7a-d** or **8a-d** (1 equiv.) were dissolved in acetonitrile and $Ba(ClO_4)_2$ (5 equiv.) was added. The resulting solution was treated with ultrasound for 5 min. Afterwards, the solvent was removed and dichloromethane was added. The mixture was stirred for 10 min and filtered. The solvent of the filtrate was removed again to yield the respective barium complexes **Ba7a-d** or **Ba8a-d**, respectively, in quantitative yields.

**Barium 25,27-bis(*N*-trifluoromethanesulfonylcarbamoylmethoxy)calix[4]arene-crown-6 (Ba7a)**

$^1$H NMR (600 MHz, $CDCl_3$): δ = 3.28 (d, $^2J$ = 13.6 Hz, 4H, $ArCH_2$), 3.79 (br. s, 4H, $OCH_2$), 3.85 (br. s, 8H, 2 x $OCH_2$), 3.90–4.00 (m, 8H, $OCH_2$), 4.54 (d, $^2J$ = 13.6 Hz, 4H, $ArCH_2$), 5.18 (s, 4H, $CH_2C$=O), 6.25–6.39 (m, 6H, *p*-$H_{Ar}$+*m*-$H_{Ar}$), 6.98 (t, $^3J$ = 7.4 Hz, 2H, *p*-$H_{Ar}$), 7.13 (d, $^3J$ = 7.4 Hz, 4H, *m*-$H_{Ar}$). $^{13}$C NMR (151 MHz, $CDCl_3$): δ = 31.7 ($ArCH_2$), 68.9, 70.0, 70.1, 70.3 (4 x $OCH_2$), 70.5 ($\underline{C}H_2C$=O), 73.0 ($OCH_2$), 119.3 (q, $^1J_{C,F}$ = 321.6 Hz, $CF_3$), 123.2, 123.7 (2 x *p*-$C_{Ar}$), 128.1, 129.3 (2 x *m*-$C_{Ar}$), 132.7, 136.4 (2 x *o*-$C_{Ar}$), 154.4, 154.7 (2 x *i*-$C_{Ar}$), 167.7 (C=O). $^{19}$F NMR (565 MHz, $CDCl_3$): δ = -76.2 (6F, $CF_3$).

**Barium 25,27-bis(*N*-pentafluoroethanesulfonylcarbamoylmethoxy)calix[4]arene-crown-6 (Ba7b)**

$^1$H NMR (600 MHz, $CDCl_3$): δ = 3.29 (d, $^2J$ = 13.5 Hz, 4H, $ArCH_2$), 3.80 (br. s, 4H, $OCH_2$), 3.86 (br. s, 8H, 2 x $OCH_2$), 3.93 (br. s, 4H, $OCH_2$), 3.96-4.00 (m, 4H, $OCH_2$), 4.56 (d, $^2J$ = 13.5 Hz, 4H, $ArCH_2$), 5.20 (s, 4H, $CH_2C$=O), 6.25-6.37 (m, 6H, *p*-$H_{Ar}$+*m*-$H_{Ar}$), 6.98 (t, $^3J$ = 7.4 Hz, 2H, *p*-$H_{Ar}$), 7.14 (d, $^3J$ = 7.4 Hz, 4H, *m*-$H_{Ar}$). $^{13}$C NMR (151 MHz, $CDCl_3$): δ = 31.7 ($ArCH_2$), 68.7, 70.0, 70.1, 70.3 (4 x $OCH_2$), 70.4 ($\underline{C}H_2C$=O), 72.8 ($OCH_2$), 123.2, 123.6 (2 x *p*-$C_{Ar}$), 128.0, 129.3 (2 x *m*-$C_{Ar}$), 132.8, 136.4 (2 x *o*-$C_{Ar}$), 154.4, 154.8 (2 x *i*-$C_{Ar}$), 167.5 (C=O). $^{19}$F NMR (565 MHz, $CDCl_3$): δ = -115.1 (4F, $CF_2$), -78.9 (6F, $CF_3$).

**Barium 25,27-bis(*N*-heptafluoropropane-2-sulfonylcarbamoylmethoxy)calix[4]arene-crown-6 (Ba7c)**

$^1$H NMR (600 MHz, $CDCl_3$): δ = 3.29 (d, $^2J$ = 13.4 Hz, 4H, $ArCH_2$), 3.80-3.88 (m, 12H, 3 x $OCH_2$), 3.93 (br. s, 4H, $OCH_2$), 3.98 (br. s, 4H, $OCH_2$), 4.60 (d, $^2J$ = 13.4 Hz, 4H, $ArCH_2$), 5.23 (s, 4H, $CH_2C$=O), 6.25-6.37 (m, 4H, *p*-$H_{Ar}$+*m*-$H_{Ar}$), 6.97 (t, $^3J$ = 7.2 Hz, 2H, *p*-$H_{Ar}$), 7.12 (d, $^3J$ = 7.2 Hz, 4H, *m*-$H_{Ar}$). $^{13}$C NMR (151 MHz, $CDCl_3$): δ = 31.7 ($ArCH_2$), 68.3, 69.9, 70.1, 70.4 (4 x $OCH_2$), 70.4 ($\underline{C}H_2C$=O), 72.4 ($OCH_2$), 123.1, 123.5 (2 x *p*-$C_{Ar}$), 128.0, 129.2 (2 x *m*-$C_{Ar}$), 132.8, 136.3 (2 x *o*-$C_{Ar}$), 154.5, 154.8 (2 x *i*-$C_{Ar}$), 176.2 (C=O). $^{19}$F NMR (565 MHz, $CDCl_3$): δ = -167.8 (2F, CF), -72.1 (12F, $CF_3$).

**Barium 25,27-bis(*N*-nonafluorobutane-1-sulfonylcarbamoylmethoxy)calix[4]arene-crown-6 (Ba7d)**

$^1$H NMR (600 MHz, $CDCl_3$): δ = 3.43 (d, $^2J$ = 12.5 Hz, 4H, $ArCH_2$), 3.83-3.90 (m, 8H, 3 x $OCH_2$), 4.02-4.08 (m, 4H, $OCH_2$), 4.14 (s, 4H, $OCH_2$), 4.37-4.47 (m, 12H, $OCH_2$+$ArCH_2$+$CH_2C$=O), 6.82 (t, $^3J$ = 7.7 Hz, 2H, *p*-$H_{Ar}$), 6.94 (t, $^3J$ = 7.6 Hz, 2H, *p*-$H_{Ar}$), 7.05 (d, $^3J$ =

7.7 Hz, 4H, *m*-$H_{Ar}$), 7.20 (d, $^3J$ = 7.6 Hz, 4H, *m*-$H_{Ar}$). $^{13}$C NMR (151 MHz, $CDCl_3$): δ = 29.5 ($ArCH_2$), 67.0, 69.1, 71.1, 71.5 (4 x $OCH_2$), 77.3 ($\underline{C}H_2C$=O), 79.7 ($OCH_2$), 126.3, 126.5 (2 x *p*-$C_{Ar}$), 129.4, 129.7 (2 x *m*-$C_{Ar}$), 134.4, 135.4 (2 x *o*-$C_{Ar}$), 152.1, 154.3 (2 x *i*-$C_{Ar}$), 175.6 (C=O). $^{19}$F NMR (565 MHz, $CDCl_3$): δ = -125.9 (4F, $CF_2$), -121.1 (4F, $CF_2$), 113.8 (4F, $CF_2$), -80.8 (6F, $CF_3$).

**Barium 5,11,17,23-tetrakis(*tert*-butyl)-25,27-bis(*N*-pentafluoroethanesulfonylcarbamoylmethoxy)calix[4]arene-crown-6 (Ba8b)**

$^1$H NMR (600 MHz, $CDCl_3$): δ = 0.92 (s, 18H, $CH_3$), 1.28 (s, 18H, $CH_3$), 3.32 (d, $^2J$ = 12.6 Hz, 4H, $ArCH_2$), 3.78-3.82 (m, 4H, $OCH_2$), 3.85.3.89 (m, 4H, $OCH_2$), 4.01-4.05 (m, 4H, $OCH_2$), 4.13 (s, 4H, $OCH_2$), 4.31 (d, $^3J$ = Hz, 4H, $ArCH_2$), 4.33-4.37 (m, 4H, $OCH_2$), 4.47 (s, 4H, $CH_2C$=O), 6.85 (s, 4H, *m*-$H_{Ar}$), 7.21 (s, 4H, *m*-$H_{Ar}$). $^{13}$C NMR (151 MHz, $CDCl_3$): δ = 29.8 ($ArCH_2$), 31.1, 31.6 (2 x $CH_3$), 34.1, 34.4 ($C_q$), 66.5, 68.9, 70.8, 71.4, (4 x $OCH_2$), 77.0 ($\underline{C}H_2C$=O), 78.8 ($OCH_2$), 126.0, 126.3 (2 x *m*-$C_{Ar}$), 133.2, 134.8 (2 x *o*-$C_{Ar}$), 147.7, 148.2 (2 x *p*-$C_{Ar}$), 148.3, 152.3 (2 x *i*-$C_{Ar}$), 176.0 (C=O). $^{19}$F NMR (565 MHz, $CDCl_3$): δ = -117.8 (4F, $CF_2$), -79.0 (6F, $CF_3$).

**Barium 5,11,17,23-tetrakis(*tert*-butyl)-25,27-bis(*N*-heptafluoropropane-2-sulfonylcarbamoylmethoxy)calix[4]arene-crown-6 (Ba8c)**

$^1$H NMR (600 MHz, $CDCl_3$): δ = 0.93 (s, 18H, $CH_3$), 1.28 (s, 18H, $CH_3$), 3.32 (d, $^2J$ = 12.6 Hz, 4H, $ArCH_2$), 3.77-3.82 (m, 4H, $OCH_2$), 3.84-3.89 (m, 4H, $OCH_2$), 4.00-4.05 (m, 4H, $OCH_2$), 4.13 (s, 4H, $OCH_2$), 4.28-4.37 (m, 8H, $OCH_2$+$ArCH_2$), 4.45 (s, 4H, $CH_2C$=O), 6.85 (s, 4H, *m*-$H_{Ar}$), 7.21 (s, 4H, *m*-$H_{Ar}$). $^{13}$C NMR (151 MHz, $CDCl_3$): δ = 29.7 ($ArCH_2$), 31.1, 31.7 (2 x $CH_3$), 34.1, 34.4 ($C_q$), 66.5, 69.0, 70.9, 71.5, 77.0 (5 x $OCH_2$), 77.4 ($\underline{C}H_2C$=O), 78.8 ($OCH_2$), 126.0, 126.3 (2 x *m*-$C_{Ar}$), 133.2, 134.9 (2 x *o*-$C_{Ar}$), 147.7, 148.3 (2 x *p*-$C_{Ar}$), 148.4, 152.2 (2 x *i*-$C_{Ar}$), 175.7 (C=O). $^{19}$F NMR (565 MHz, $CDCl_3$): δ = -171.1 (2F, CF), -71.7 (12F, $CF_3$).

**Barium 5,11,17,23-tetrakis(*tert*-butyl)-25,27-bis(*N*-nonafluorobutane-1-sulfonylcarbamoylmethoxy)calix[4]arene-crown-6 (Ba8d)**

$^1$H NMR (600 MHz, $CDCl_3$): δ = 0.93 (s, 18H, $CH_3$), 1.28 (s, 18H, $CH_3$), 3.32 (d, $^2J$ = 12.6 Hz, 4H, $ArCH_2$), 3.77-3.81 (m, 4H, $OCH_2$), 3.84-3.88 (m, 4H, $OCH_2$), 4.01-4.05 (m, 4H, $OCH_2$), 4.12 (s, 4H, $OCH_2$), 4.28-4.37 (m, 8H, $OCH_2$+$ArCH_2$), 4.47 (s, 4H, $CH_2C$=O), 6.85 (s, 4H, m-$H_{Ar}$), 7.21 (s, 4H, m-$H_{Ar}$). $^{13}$C NMR (151 MHz, $CDCl_3$): δ = 29.8 ($ArCH_2$), 31.1, 31.7 (2 x $CH_3$), 34.1, 34.4 ($C_q$), 66.5, 68.9, 70.8, 71.4, 78.8 (5 x $OCH_2$), 126.0, 126.3 (2 x *m*-$C_{Ar}$), 133.2, 134.8 (2 x *o*-$C_{Ar}$), 147.7, 148.3 (2 x *p*-$C_{Ar}$), 148.4, 152.3 (2 x *i*-$C_{Ar}$), 176.1 (C=O). $^{19}$F NMR (565 MHz, $CDCl_3$): δ = -125.9 (4F, $CF_2$), -121.1 (4F, $CF_2$), -113.7 (4F, $CF_2$), -80.8 (6F, $CF_3$).

**Synthesis of the ion-free ligands**

The respective sodium complexes **Na7a-d** or **Na8a-d** (10-30 mg) were dissolved in chloroform (10-15 mL), aqueous HCl (10-15 mL, 10%) was added and the mixture was shaken for 10 min. Afterwards, the organic phase was separated and washed with water (2 x 10 mL). After separation of the organic phase, the solvent was removed to yield the respective ion-free ligands **L7a,b,d** or **L8a-d**, respectively, in quantitative yields.

**25,27-Bis(*N*-trifluoromethanesulfonylcarbamoylmethoxy)calix[4]arene-crown-6 (L7a)**

$^1$H NMR (600 MHz, $CDCl_3$): δ = 3.29 (d, 4H, $^2J$ = 13.5 Hz, $CH_2Ar$), 3.67-3.82 (m, 4H, $OCH_2$), 3.83-3.89 (m, 8H, $OCH_2$), 3.91-4.01 (m, 8H, $OCH_2$), 4.55 (d, 4H, $^2J$ = 13.5 Hz, $CH_2Ar$), 5.19 (s, 4H, $CH_2$), 6.24-6.36 (m, 6H, Ar-H), 6.99 (t, $^3J$ = 7.4 Hz, 2H, Ar-H), 7.14 (d, $^3J$ = 7.4 Hz, 4H, Ar-H), 11.02 ppm (s, 2H, NH); $^{13}$C NMR (151 MHz, $CDCl_3$): δ = 31.7 ($CH_2Ar$), 68.9, 69.9, 70.1, 70.3, 70.4, 72.9 (6 x $CH_2$), 119.3 (q, $^1J_{C,F}$ = 322 Hz, $CF_3$), 123.2, 123.7, 128.0, 129.3 (4 x $CH_{Ar}$), 132.7, 136.4, 154.4, 154.7 (4 x $C_{q\text{-}Ar}$), 176.7 ppm (C=O); $^{19}$F NMR (565 MHz, $CDCl_3$): δ = -76.2 ppm (6F, $CF_3$).

**25,27-Bis(*N*-pentafluoroethanesulfonylcarbamoylmethoxy)calix[4]arene-crown-6 (L7b)**

$^1$H NMR (400 MHz, $CDCl_3$): δ = 3.29 (d, 4H, $^2J$ = 13.5 Hz, $CH_2Ar$), 3.80 (br. s, 4H, $OCH_2$), 3.86 (br. s, 8H, $OCH_2$), 3.91-4.01 (m, 8H, $OCH_2$), 4.56 (d, 4H, $^2J$ = 13.5 Hz, $CH_2Ar$), 5.21 (s, 4H, $CH_2$), 6.25-6.37 (m, 6H, Ar-H), 6.98 (t, $^3J$ = 7.5 Hz, 2H, Ar-H), 7.14 (d, $^3J$ = 7.5 Hz, 4H, Ar-H), 11.03 ppm (s, 2H, NH); $^{13}$C NMR (101 MHz, $CDCl_3$): δ = 31.7 ($CH_2Ar$), 68.8, 70.0, 70.1, 70.3, 70.4, 72.8 (6 x $CH_2$), 119.3 (q, $^1J_{C,F}$ = 322 Hz, $CF_3$), 123.2, 123.6, 128.0, 129.3 (4 x $CH_{Ar}$), 132.8, 136.4, 154.4, 154.7 (4 x $C_{q\text{-}Ar}$), 176.5 ppm (C=O); $^{19}$F NMR (376 MHz, $CDCl_3$): δ = -115.1 (4F, $CF_2$), -78.9 ppm (6F, $CF_3$).

**25,27-Bis(*N*-nonafluorobutane-1-sulfonylcarbamoylmethoxy)calix[4]arene-crown-6 (L7d)**

$^1$H NMR (600 MHz, $CDCl_3$): δ = 3.28 (d, 4H, $^2J$ = 13.4 Hz, $CH_2Ar$), 3.67-3.82 (m, 4H, $OCH_2$), 3.83-3.89 (m, 8H, $OCH_2$), 3.91-4.01 (m, 8H, $OCH_2$), 4.56 (d, 4H, $^2J$ = 13.4 Hz, $CH_2Ar$), 5.20 (s, 4H, $CH_2$), 6.25-6.34 (m, 6H, Ar-H), 6.98 (t, $^3J$ = 7.4 Hz, 2H, Ar-H), 7.13 (d, $^3J$ = 7.4 Hz, 4H, Ar-H), 11.00 ppm (s, 2H, NH). $^{13}$C NMR (151 MHz, $CDCl_3$): δ = 31.7 ($CH_2Ar$), 68.7, 69.9, 70.0, 70.4, 70.5, 72.7 (6 x $CH_2$), 123.2, 123.6, 128.0, 129.3 (4 x $CH_{Ar}$), 132.8, 136.4, 154.4, 154.8 (4 x $C_{q\text{-}Ar}$), 176.4 ppm (C=O); $^{19}$F NMR (565 MHz, $CDCl_3$): δ = -125.8 (4F, $CF_2$), -121.2 (4F, $CF_2$), -110,9 (4F, $CF_2$), -80.7 ppm (6F, $CF_3$).

**5,11,17,23-Tetrakis(*tert*-butyl)-25,27-bis(*N*-trifluoromethanesulfonylcarbamoylmethoxy)calix[4]arene-crown-6 (L8a)**

$^1$H NMR (600 MHz, $CDCl_3$): δ = 0.82 (s, 18 H, $^t$Bu), 1.34 (s, 18 H, $^t$Bu), 3.38 (d, 4 H, $^2J$ = 13.1 Hz, $CH_2Ar$), 3.75-3.98 (m, 20H, $OCH_2$), 4.52 (br. s, 4H, $CH_2Ar$), 5.24 (s, 4 H, $CH_2CO$), 6.46 (s, 4 H, ArH), 7.10 (s, 4 H, ArH), 11.03 ppm (br. s, 2H, NH); $^{13}$C NMR (151 MHz, $CDCl_3$): δ = 31.2, 31.8 (2 x $^t$Bu), 32.2 ($CH_2Ar$), 33.8, 34.2 (2 x $C_q$), 68.9, 70.3, 70.6, 73.6 (4 x $CH_2$), 119.3 (q, $^1J_{C,F}$ = 322.1 Hz, $CF_3$), 124.9, 126.0 (2 x $CH_{Ar}$), 131.7, 135.2, 145.3, 146.1, 151.6, 152.6 (6 x $C_{q\text{-}Ar}$), 168.2 ppm (C=O); $^{19}$F NMR (565 MHz, $CDCl_3$): δ = -76.1 (6F, $CF_3$) ppm.

**5,11,17,23-Tetrakis(*tert*-butyl)-25,27-bis(*N*-pentafluoroethanesulfonylcarbamoylmethoxy)calix[4]arene-crown-6 (L8b)**

$^1$H NMR (600 MHz, $CDCl_3$): δ = 0.81 (s, 18H, $CH_3$), 1.33 (s, 18H, $CH_3$), 3.24 (d, $^2J$ = 13.3 Hz, 4H, $ArCH_2$), 3.76–3.93 (m, 20H, $OCH_2$), 4.53 (br. s, 4H, $ArCH_2$), 5.25 (s, 4H, $CH_2C$=O), 6.46 (s, 4H, *m*-$H_{Ar}$), 7.10 (s, 4H, *m*-$H_{Ar}$), 11.03 (br. s, 2H, NH). $^{13}$C NMR (151 MHz, $CDCl_3$): δ = 31.2, 31.8 (2 x $CH_3$), 32.2 ($ArCH_2$), 33.8, 34.2 ($C_q$), 68.8, 70.0, 70.3, 70.7, 73.4 (5 x $OCH_2$), 70.2 ($\underline{C}H_2C$=O), 124.9, 126.0 (2 x *m*-$C_{Ar}$), 131.7, 135.2 (2 x *o*-$C_{Ar}$), 145.2, 146.1 (2 x *p*-$C_{Ar}$), 152.6, 152.7 (2 x *i*-$C_{Ar}$), 168.0 (C=O). $^{19}$F NMR (565 MHz, $CDCl_3$): δ = -117.8 (4F, $CF_2$), -79.0 ppm (6F, $CF_3$).

**5,11,17,23-Tetrakis(*tert*-butyl)-25,27-bis(*N*-heptafluoropropane-2-sulfonylcarbamoylmethoxy)calix[4]arene-crown-6 (L8c)**

$^1$H NMR (600 MHz, $CDCl_3$): δ = 0.82 (s, 18 H, $^t$Bu), 1.33 (s, 18 H, $^t$Bu), 3.25 (d, 4 H, $^2J$ = 13.0 Hz, $CH_2Ar$), 3.78–3.99 (m, 20H, $OCH_2$), 4.58 (br. s, 4H, $CH_2Ar$), 5.26 (s, 4 H, $CH_2CO$), 6.47 (s, 4 H, ArH), 7.10 (s, 4 H, ArH), 10.98 ppm (br. s, 2H, NH); $^{13}$C NMR (151 MHz, $CDCl_3$): δ = 31.2, 31.7 (2 x $^t$Bu), 32.2 ($CH_2Ar$), 33.8, 34.2 (2 x $C_q$), 68.7, 70.0, 70.3, 70.6 (5 x $OCH_2$), 70.2 ($\underline{C}H_2C$=O), 124.9, 126.0 (2 x *m*-$C_{Ar}$), 131.8, 135.1 (2 x *o*-$C_{Ar}$), 145.3, 145.6 (2 x *p*-$C_{Ar}$), 151.2, 152.4 (2 x *i*-$C_{Ar}$), 167.7 ppm (C=O); $^{19}$F NMR (565 MHz, $CDCl_3$): δ = -168.2 (2F, CF), -71.5 ppm (12F, $CF_3$).

**5,11,17,23-Tetrakis(*tert*-butyl)-25,27-bis(*N*-nonafluorobutane-1-sulfonylcarbamoylmethoxy)calix[4]arene-crown-6 (L8d)**

$^1$H NMR (400 MHz, $CDCl_3$): δ = 0.81 (s, 18 H, $^t$Bu), 1.33 (s, 18 H, $^t$Bu), 3.25 (d, 4 H, $^2J$ = 13.1 Hz, $CH_2Ar$), 3.78–3.98 (m, 20H, $OCH_2$), 4.54 (br. s, 4H, $CH_2Ar$), 5.26 (s, 4 H, $CH_2CO$), 6.46 (s, 4 H, ArH), 7.10 (s, 4 H, ArH), 11.01 ppm (br. s, 2H, NH); $^{13}$C NMR (101 MHz, $CDCl_3$): δ = 31.2, 31.8 (2 x $^t$Bu), 32.2 ($CH_2Ar$), 33.8, 34.2 (2 x $C_q$), 68.8, 70.1, 70.4, 70.6, 73.4 (5 x $OCH_2$), 70.2 ($\underline{C}H_2C$=O), 124.9, 126.1 (2 x *m*-$C_{Ar}$), 131.7, 135.2 (2 x *o*-$C_{Ar}$), 145.3, 146.0 (2 x *p*-$C_{Ar}$), 151.7, 152.7 (2 x *i*-$C_{Ar}$), 167.9 ppm (C=O); $^{19}$F NMR (376 MHz, $CDCl_3$): δ = -125.9 (4F, $CF_2$), -121.2 (4F, $CF_2$), -111.0 (4F, $CF_2$), -80.7 ppm (6F, $CF_3$).

**Extraction experiments with $[^{133}Ba]BaCl_2$ and $[^{224}Ra]Ra(NO_2)_2$**

All ligands were dissolved in 600 µL chloroform adjusted to the respective ligand concentration. An approximate activity amount of 50 kBq ($[^{133}Ba]BaCl_2$ or $[^{224}Ra]Ra(NO_2)_2$) was added in 600 µL of water to the ligand-containing chloroform phase. The aqueous solution was extracted in an overhead shaker for 1 h at rt. After each extraction was finished, an equivalent volume of both phases was taken to measure the activity (count rates) of the both the aqueous and the organic phase using a sodium iodide detector ISOMED2160.

In order to examine the selectivity and stability of the barium and radium complexes against calcium ions, an equivalent volume of the complex-containing chloroform solution was taken and extracted with a 1% (m/m) $CaCl_2$ solution for 1 h at rt. After each extraction was finished, an equivalent volume of both phases was taken to measure the activity (count rates) of the both the aqueous and the organic phase using a sodium iodide detector ISOMED2160.

## Conclusions

A series of calix[4]arenes with sulfonamide functions was synthesized which were used as chelators for $Ba^{2+}$ and $Ra^{2+}$ to determine the complexation behavior of these two ions. For this purpose, the respective metal ion-free ligands, Na- and Ba-complexes were characterized. Furthermore, an extraction method was established to determine the association constants using $[^{133}Ba]Ba^{2+}$ and $[^{224}Ra]Ra^{2+}$ pointing out an introduction of these ions by easy replacement of $Na^+$. These findings were further supported by additional DFT calculations to explain the binding behavior of $Ba^{2+}$ and $Ra^{2+}$. Additional challenge experiments with the radiolabeled complexes and $Ca^{2+}$ were performed showing only a minor release of activity. In summary, the deprotonatable side functions together with a crown ether structure connected to the calixarene skeleton are the basis for considerable complex stability resulting in high association constants, but there is still room to improve the stability of these complexes for future application as chelators in radiopharmacy.

## Conflicts of interest

There are no conflicts to declare.

## Acknowledgements

The authors thank Linda Belke for her extensive experimental support.

## References

1 C. D. Gutsche, Calixarenes: An Introduction, Vol. 2, The Royal Society of Chemistry, Cambridge, 2008.
2 W. Sliwa, C. Kozlowski, Calixarenes and Resorcinarenes, Wiley-VCH, Weinheim, 2009.
3 R. Gramage-Doria, D. Armspach and D. Matt, Metallated cavitands (calixarenes, resorcinarenes, cyclodextrins) with internal coordination sites. *Coord. Chem. Rev.,* 2013, **257**, 776.
4 S. B. Nimse and T. Kim, Biological applications of functionalized calixarenes. *Chem. Soc. Rev.,* 2013, **42**, 366.
5 R. Zadmard and N. S. Alavijeh, Protein surface recognition by calixarenes. *RSC Adv.,* 2014, **4**, 41529.
6 C. Deraedt and D. Astruc, Supramolecular nanoreactors for catalysis. *Coord. Chem. Rev.,* 2016, **324**, 106.
7 D. Sémeril and D. Matt, Synthesis and catalytic relevance of P(III) and P(V)-functionalised calixarenes and resorcinarenes. *Coord. Chem. Rev.,* 2014, **279**, 58.
8 D. M. Homden and C. Redshaw, The Use of Calixarenes in Metal-Based Catalysis. *Chem. Rev.,* 2008, **108**, 5086.
9 S. Siddiqui and P. J. Cragg, Design and Synthesis of Transition Metal and Inner Transition Metal Binding Calixarenes. *Mini-Rev. Org. Chem.,* 2009, **6**, 283.
10 E. A. Shokova and V. V. Kovalev, Calixarene-based anionic receptors. *Russ. J. Org. Chem.,* 2009, **45**, 1275.
11 B. Mokhtari and K. Pourabdollah, Application of Calixarenes in Development of Sensors. *Asian J. Chem.,* 2013, **25**, 1.
12 U. Ocak, M. Ocak and R. A. Bartsch, Calixarenes with dansyl groups as potential chemosensors. *Inorg. Chim. Acta,* 2012, **381**, 44.

13 J. L. Atwood in Cation Binding by Macrocycles-Complexation of Cationic Species by Crown Ethers, Vol. 15 (Eds.: Y. Inoue, G. W. Gokel), Marcel Dekker, New York, NJ, 1990, pp. 581–598.
14 G. W. Gokel in Comprehensive Supramolecular Chemistry II, Vol. 1 (Eds.: G. W. Gokel, L. Barbour), Elsevier, Amsterdam, Oxford, Cambridge, 2017, pp. 203–216.
15 M. L. Dietz, R. Chiarizia, E. P. Horwitz, R. A. Bartsch and V. Talanov, Effect of crown ethers on the ion-exchange behavior of alkaline Earth metals. Toward improved ion-exchange methods for the separation and preconcentration of radium . *Anal. Chem.,* 1997, **69**, 3028.
16 Z. Asfari, B. Pulpoka, M. Saadioui, S. Wenger, M. Nierlich, P. Thuery, N. Reynier, J. F. Dozol, J. Vicens in Molecular Recognition and Inclusion. Proceedings of the Ninth International Symposium on Molecular Recognition and Inclusion, (Ed.: A. W. Coleman), Springer, Dordrecht, 1998, 173–178.
17 R. Sharma and E. Aboagye, Development of radiotracers for oncology-the interface with pharmacology. *Br. J. Pharmacol.,* 2011, **163**, 1565.
18 M. Fani, S. Good, H. R. Mäcke in Handbook of Nuclear Chemistry, Vol. 4 (Eds.: A. Vértes, S. Nagy, Z. Klencsàr, R. G. Lovas, F. Rösch), Springer, Dordrecht, Heidelberg, London, New York, 2011, pp. 2143–2178.
19 N. A. Thiele, S. N. MacMillan and J. J. Wilson, Rapid Dissolution of $BaSO_4$ by Macropa, an 18-Membered Macrocycle with High Affinity for $Ba^{2+}$. J. Am. Chem. Soc., 2018, 140, 17071-17078.
20 G. Henriksen, P. Hoff and R. H. Larsen, Evaluation of potential chelating agents for radium. *Appl. Radiat. Isot.*, 2002, **56**, 667-671.
21 M. Freesmeyer, W. Weigand and T. Weisheit, Examination of the complexation ability of different calixarene derivatives towards $[^{223}Ra]RaCl_2$ in a hospital radiopharmaceutical laboratory. *Nuklearmedizin*, 2018, **57**, 242-246.
22 A. S. Ivanov, M. E. Simms, V. S. Bryantsev, P. D. Benny, J. R. Griswold, L. H. Delmau and N. A. Thiele, Elucidating the coordination chemistry of the radium ion for targeted alpha therapy. *Chem. Commun.*, 2022, **58**, 9938-9941.
23 T.-C. Wun, R. Bittman and I. J. Borowitz, Binding properties of neutral diamide ligands for alkaline-earth cations. *Biochemistry,* 1977, **16**, 2074.
24 X. Y. Chen, M. Ji, D. R. Fisher and C. M. Wai, Ionizable Calixarene-Crown Ethers with High Selectivity for Radium over Light Alkaline Earth Metal Ions. *Inorg. Chem.,* 1999, **38**, 5449.
25 F. Reissig, K. Kopka and C. Mamat, The impact of barium isotopes in radiopharmacy and nuclear medicine - From past to presence. *Nucl. Med. Biol.,* 2021, **98**, 59.
26 F. Reissig, K. Kopka and C. Mamat, Die Bedeutung des Elementes Barium in der Nuklearmedizin. *Der Nuklearmediziner,* 2021, **44**, 127.
27 F. Reissig, D. Bauer, M. Ullrich, M. Kreller, C. Mamat, J. Pietzsch, K. Kopka, H.-J. Pietzsch and M. Walther, Recent Insights in Barium-131 as a Diagnostic Match for Radium-223: Cyclotron Production, Separation, Radiolabeling, and Imaging. *Pharmaceuticals,* 2020, **13**, 272.
28 J. Steinberg, D. Bauer, F. Reissig, H.-J. Pietzsch and C. Mamat, Modified Calix[4]crowns as Molecular Receptors for Barium. *ChemistryOpen* 2018, **7**, 432.
29 D. Bauer, M. Gott, J. Steinbach and C. Mamat, Chelation of heavy group 2 (radio)metals by *p-tert*-butylcalix[4]arene-1,3-crown-6 and logK determination *via* NMR. *Spectrochim. Acta A,* 2018, **199**, 50.
30 D. Bauer, M. Blumberg, M. Köckerling and C. Mamat, A comparative evaluation of calix[4]arene-1,3-crown-6 as a ligand for selected divalent cations of radiopharmaceutical interest. *RSC Adv.,* 2019, **9**, 32357.
31 M. Blumberg, K. Al-Ameed, E. Eiselt, S. Luber and C. Mamat, Synthesis of Ionizable Calix[4]arenes for Chelation of Selected Divalent Cations. *Molecules,* 2022, **27**, 1478.
32 M. Gott, J. Steinbach and C. Mamat, The Radiochemical and Radiopharmaceutical Applications of Radium. *Open Chem.,* 2016, **14**, 118.
33 P. L. Brown, A. V. Matyskin, and C. Ekberg, The aqueous chemistry of radium. *Radiochim. Acta,* 2022, **110**, 505.
34 D. S. Abou, N. A. Thiele, N. T. Gutsche, A. Villmer, H. Zhang, J. J. Woods, K. E. Baidoo, F. E. Escorcia, J. J. Wilson and D. L. J. Thorek, Towards the stable chelation of radium for biomedical applications with an 18-membered macrocyclic ligand. *Chem Sci.*, 2021, **12**, 3733-3742.
35 P. M. Colletti, *Clin. Nucl. Med.,* 2013, **38**, 724.
36 D. Bauer, F. Reissig, H.-J. Pietzsch, J. Steinbach and C. Mamat, Calixarene Based Ligands for Radium and Barium. *J. Med. Imaging Radiat. Sci.,* 2018, **50**, S39.
37 N. Drude, L. Tienken and F. M. Mottaghy, Theranostic and nanotheranostic probes in nuclear medicine. *Methods,* 2017, **130**, 14.
38 L. Davis, A.-L. Smith, M. D. Aldridge, J. Foulkes, C. Peet, S. Wan, J. E. Gains, J. B. Bomanji and M. N. Gaze, Personalisation of Molecular Radiotherapy through Optimisation of Theragnostics. *J. Pers. Med.,* 2020, **10**, 174.
39 F. W. van Leeuwen, H. Beijleveld, C. J. Miermans, J. Huskens, W. Verboom and D. N. Reinhoudt, Ionizable (Thia)calix[4]crowns as Highly Selective $^{226}Ra^{2+}$ Ionophores. *Anal. Chem.,* 2005, **77**, 4611.
40 F. W. B. van Leeuwen, W. Verboom and D. N. Reinhoudt, Selective extraction of naturally occurring radioactive $Ra^{2+}$. *Chem. Soc. Rev.,* 2005, **34**, 753.
41 C. Tu, K. Surowiec, J. Gega, D. W. Purkiss and R. A. Bartsch, Di-ionizable p-tert-butylcalix[4]arene-1,2-crown-5 ligands in the cone conformation: effect of acidic side arm length for solvent extraction of divalent metal ions. *Tetrahedron,* 2008, **64**, 1187.
42 H. Zhou, K. Surowiec, D. W. Purkiss and R. A. Bartsch, Proton di-ionizable p-tert-butylcalix[4]arene-crown-6 compounds in cone, partial-cone and 1,3-alternate conformations: synthesis and alkaline earth metalcation extraction. *Org. Biomol. Chem.,* 2005, **3**, 1676.
43 H. Zhou, D. Liu, J. Gega, K. Surowiec, D. W. Purkiss, and R. A. Bartsch, Effect of *para*-substituents on alkaline earth metal ion extraction by proton di-ionizable calix[4]arene-crown-6 ligands in cone, partial-cone and 1,3-alternate conformations. *Org. Biomol. Chem.,* 2007, **5**, 324.
44 A. L. Boston, E. K. Lee, K. Surowiec, J. Gega and R. A. Bartsch, Comparison of upper and lower rim-functionalized, di-ionizable calix[4]arene-crown-6 structural isomers in divalent metal ion extraction. *Tetrahedron,* 2012, **68**, 8789.
45 J. W. Akitt in Multinuclear NMR, Plenum Press, New York, 1987, Chapt. 7
46 Calculations by ChemDraw Professional, Version: 17.0.0.206 (121), PerkinElmer 1998-2017.
47 R. D. Shannon, Revised effective ionic radii and systematic studies of interatomic distances in halides and chalcogenides. *Acta Cryst.,* 1976, **A32**, 751.
48 K. Hirose, *Quantitative Analysis of Binding Properties* in Analytical Methods in Supramolecular Chemistry (Ed.: C. A. Schalley), Wiley-VCH Verlag Weinheim, 2006, pp. 17-54.
49 H.-J. Schneider, H. Dürr, Frontiers in supramolecular organic chemistry and photochemistry, VCH, Weinheim, 1991.
50 G. Weber, in Molecular Biophysics (Eds.: B. Pullman, M. Weissbluth), Academic Press, New York, 1965, pp. 369-396.
51 S. Haupt, R. Schnorr, M. Poetsch, A. Mansel, M. Handke, B. Kersting, Extraction properties of 25,27-


 

bis(carbonylmethoxy)calix[4]arenes towards $Sr^{2+}$: competitive extraction and extraction in a synthetic groundwater. *J. Radioanal. Nucl. Chem.,* 2014, **300**, 779.
52 H. Steinbeisser and R. Mews, Additionsreaktionen mit fluorierten Diazoverbindungen: Über die Darstellung von N-Perfluorisopropyl-oxathiazolin- und S-Perfluorisopropyl-oxathiazol-Derivaten. *Z. Naturforsch. B,* 1976, **31B**, 1480.
53 F. Reissig, R. Hübner, J. Steinbach, H.-J. Pietzsch and C. Mamat, Facile preparation of radium-doped, functionalized nanoparticles as carriers for targeted alpha therapy. *Inorg. Chem. Front.,* 2019, **6**, 1341.
54 G. M. Sheldrick, Crystal structure refinement with SHELXL. *Acta Cryst. C,* 2015, **71**, 3.
55 G. M. Sheldrick, A short history of SHELX - International Union of Crystallography. *Acta Cryst. A,* 2008, **64**, 112.
56 G. M. Sheldrick, SHELXL 2014, University of Göttingen, Germany, 2014.
57 J. P. Perdew, Density-functional approximation for the correlation energy of the inhomogeneous electron gas. *Phys. Rev. B,* 1986, **33**, 8822.
58 A. D. Becke, Density-functional exchange-energy approximation with correct asymptotic behavior. *Phys. Rev. A,* 1988, **38**, 3098.
59 A. D. Becke, Density-functional thermochemistry. III. The role of exact exchange. *J. Chem. Phys.,* 1993, **98**, 5648.
60 C. Lee, W. Yang and R. G. Parr, Development of the Colle-Salvetti correlation-energy formula into a functional of the electron density. *Phys. Rev. B* 1988, **37**, 785.
61 K. Eichkorn, O. Treutler, H. Ohm, M. Häser and R. Ahlrichs, Auxiliary basis sets to approximate Coulomb potentials. *Chem. Phys. Lett.,* 1995, **240**, 283.
62 F. Weigend, A fully direct RI-HF algorithm: Implementation, optimised auxiliary basis sets, demonstration of accuracy and efficiency. *Phys. Chem. Chem. Phys.,* 2002, **4**, 4285.
63 S. Grimme, J. Anthony, S. Ehrlich and H. Krieg, A consistent and accurate ab initio parametrization of density functional dispersion correction (DFT-D) for the 94 elements H-Pu. *J. Chem. Phys.*, 2010, **132**, 154104.
64 K. Eichkorn, F. Weigend, O. Treutler and R. Ahlrichs, Optimized accurate auxiliary basis sets for RI-MP2 and RI-CC2 calculations for the atoms Rb to Rn. *Theor. Chem. Acc.*, 1997, **97**, 119.
65 R. Ahlrichs, M. Bär, M. Häser, H. Horn and C. Kölmel, Electronic structure calculations on workstation computers: The program system turbomole. *Chem. Phys. Lett.,* 1989, **62**,165.
66 A. Klamt, F. Eckert, M. Diedenhofen and M. E. Beck, First Principles Calculations of Aqueous pKa Values for Organic and Inorganic Acids Using COSMO-RS Reveal an Inconsistency in the Slope of the pKa Scale. *J. Phys. Chem. A,* 2003, **107**, 9380.